THE JOURNAL OF BIOLOGICAL CHEMISTRY VOL. 283, NO. 36, pp. 24718–24728, September 5, 2008


# The PDZ and Band 4.1 Containing Protein Frmpd1 Regulates the Subcellular Location of Activator of G-protein Signaling 3 and Its Interaction with G-proteins*[S]

Received for publication, May 8, 2008, and in revised form, June 9, 2008 Published, JBC Papers in Press, June 19, 2008, DOI 10.1074/jbc.M803497200

**Ningfei An**[‡§], **Joe B. Blumer**[‡§], **Michael L. Bernard**[§], **and Stephen M. Lanier**[‡§1]

*From the* [‡]*Department of Pharmacology and Experimental Therapeutics, Louisiana State University Health Sciences Center, New Orleans, Louisiana 70112 and the* [§]*Department of Pharmacology, Medical University of South Carolina, Charleston, South Carolina 29425*

**Activator of G-protein signaling 3 (AGS3) is one of nine mammalian proteins containing one or more G-protein regulatory (GPR) motifs that stabilize the GDP-bound conformation of $G\alpha_i$. Such proteins have revealed unexpected functional diversity for the "G-switch" in the control of events within the cell independent of the role of heterotrimeric G-proteins as transducers for G-protein-coupled receptors at the cell surface. A key question regarding this class of proteins is what controls their subcellular positioning and interaction with G-proteins. We conducted a series of yeast two-hybrid screens to identify proteins interacting with the tetratricopeptide repeat (TPR) of AGS3, which plays an important role in subcellular positioning of the protein. We report the identification of Frmpd1 (FERM and PDZ domain containing 1) as a regulatory binding partner of AGS3. Frmpd1 binds to the TPR domain of AGS3 and coimmunoprecipitates with AGS3 from cell lysates. Cell fractionation indicated that Frmpd1 stabilizes AGS3 in a membrane fraction. Upon cotransfection of COS7 cells with Frmpd1-GFP and AGS3-mRFP, AGS3-mRFP is observed in regions of the cell cortex and also in membrane extensions or processes where it appears to be colocalized with Frmpd1-GFP based upon the merged fluorescent signals. Frmpd1 knockdown (siRNA) in Cath.a-differentiated neuronal cells decreased the level of endogenous AGS3 in membrane fractions by ~50% and enhanced the $\alpha_2$-adrenergic receptor-mediated inhibition of forskolin-induced increases in cAMP. The coimmunoprecipitation of Frmpd1 with AGS3 is lost as the amount of $G\alpha_{i3}$ in the cell is increased and AGS3 apparently switches its binding partner from Frmpd1 to $G\alpha_{i3}$ indicating that the interaction of AGS3 with Frmpd1 and $G\alpha_{i3}$ is mutually exclusive. Mechanistically, Frmpd1 may position AGS3 in a membrane environment where it then interacts with $G\alpha_i$ in a regulated manner.**

G-protein-coupled receptor systems defined by the basic core cassette of a cell-surface receptor, heterotrimeric G-protein, and effector mediate a tremendous number of signaling events within the cell. Nature achieves plasticity within this system by subtle alterations of different key steps involved in signal initiation, transfer, and propagation. Such subtle "twitching" of the system may be reflected as changes in conformational flexibility of the receptor, the affinity of $G\alpha$ for $G\beta\gamma$, or the positioning of the protein within the cell. Accessory proteins that influence signal initiation or transfer within the system also play important roles in the regulatory processes. Such proteins have revealed unexpected functional diversity for the "G-switch" in the control of events within the cell independent of the role of heterotrimeric G-proteins as transducers for G-protein-coupled receptors at the cell surface (1–3).

One group of accessory proteins for G-proteins, receptor-independent activators of G-protein signaling (AGS)[2] proteins, were identified in a yeast-based functional screen of mammalian cDNAs (1, 3–5). Group II AGS proteins (AGS3–6) each contain one or more G-protein regulatory (GPR) or GoLoco motifs that bind $G\alpha_i$, $G\alpha_t > G\alpha_o$. AGS3 (~72 kDa) and AGS5/LGN (~74 kDa), which exhibit ~59% amino acid sequence identity, each contain a series of tetratricopeptide repeats upstream of four GPR motifs with the two domains separated by a linker region (6, 7). AGS4 (17.9 kDa) contains three GPR motifs without any other defined motifs (1, 8). AGS6 is identical to a region of RGS12 that has one GPR motif (2, 9). The GPR motif stabilizes the GDP-bound conformation of $G\alpha$ essentially behaving as a guanine nucleotide dissociation inhibitor and as an alternative, regulatory binding partner for $G\alpha$ independent of $G\beta\gamma$ (6, 10–12). This property is apparently of broad functional significance as AGS3, AGS5/LGN, and other GPR containing proteins are involved in neuronal development, synaptic plasticity, cell division, and/or autophagy via G-protein signaling mechanisms across multiple organisms (1, 13–34).

Despite the strong biochemical studies defining the interaction of AGS3 and other GPR-containing proteins with $G\alpha$ and animal studies implicating diverse roles for these proteins in cellular function, we lack a complete understanding of the "stimulus input" to these proteins and the nature of the subse-

* This work was supported, in whole or in part, by National Institutes of Health Grants MH90531 (to S. M. L.), NS24821 (to S. M. L.), and F32MH65092 (to J. B. B.). The costs of publication of this article were defrayed in part by the payment of page charges. This article must therefore be hereby marked "*advertisement*" in accordance with 18 U.S.C. Section 1734 solely to indicate this fact.

[S] The on-line version of this article (available at http://www.jbc.org) contains supplemental Figs. S1–S5.

[1] Supported by a Research Scholar Award from Yamanouchi Pharmaceutical Company (now Astellas Pharma) and the Lederle Laboratories/David R. Bethune Professorship in Pharmacology at Louisiana State University Health Sciences Center, New Orleans. To whom correspondence should be addressed: Dept. of Pharmacology, Medical University of South Carolina, Charleston, SC 29425. Tel.: 843-792-7134; E-mail: lanier@musc.edu.

[2] The abbreviations used are: AGS, activators of G-protein signaling; GPR, G-protein regulatory motif; GST, glutathione *S*-transferase; siRNA, small interfering RNA; CAD, Cath.a-differentiated.

quent downstream signaling events and their integration. Key questions in the field include the following. What regulates the formation and dissociation of an AGS3-G$\alpha_i$ complex? What regulates the subcellular location of AGS3? Where does the interaction of AGS3 and G$\alpha_i$ occur within the cell? The subcellular location of GPR proteins and their interaction with G-proteins is likely determined by coordinated and regulated interaction with protein binding partners (1, 13, 21, 26, 27, 29, 30, 34–38). How signals may be initiated through these binding partners is not known, nor can the limited number of binding partners identified to date satisfactorily account for known positioning of AGS3 and other GPR proteins within the cell.

As part of a broader strategy to define potential regulatory mechanisms involved in the subcellular localization of GPR proteins and/or stimulus input for GPR-G$\alpha$ interactions, we conducted a series of yeast two-hybrid screens with the region of AGS3 containing the TPR domain (AGS3-TPR), which is likely involved in subcellular positioning of the protein (39). We report the identification of Frmpd1 (FERM and PDZ domain containing protein 1) as an AGS3-TPR domain binding partner that influences the subcellular location of AGS3 and its interaction with G-proteins.

## EXPERIMENTAL PROCEDURES

*Materials*—Human full-length Frmpd1 cDNA in pBluescript II SK(+) was obtained from the Kazusa DNA Research Institute (Kazusa-kamatari, Kisarazu, Japan) (40, 41). The cDNA was digested with KpnI and NotI and then subcloned into pcDNA3 vector purchased from Invitrogen. The pmCherryN1::AGS3 was generated by digesting pEGFPN1::AGS3 (28) with XhoI and BamHI and then subcloning the AGS3 insert into pmCherryN1 (Clontech). Lipofectamine 2000 was obtained from Invitrogen. Glutathione-Sepharose 4B and GammaBind G-Sepharose were purchased from Amersham Biosciences. G$\alpha_{i3}$ antiserum was a kind gift from Dr. Thomas Gettys (Pennington Biomedical Research Center (42). AGS3 affinity purified antibodies (PEP32) were described previously (6, 39). Monoclonal actin antibody (MAB1501R) was purchased from Chemicon International, and the glutathione *S*-transferase (GST) antibody was purchased from Amersham Biosciences. COS7 cells were purchased from American Type Culture Collection (ATCC) (Manassas, VA) and Cath.a-differentiated (CAD) cells were generously provided by Dr. James Bear (University of North Carolina, Chapel Hill, NC). COS7 cells were grown in Dulbecco's modified Eagle's medium with 10% fetal bovine serum and 1% penicillin/streptomycin solution (Cellgro). CAD cells were grown in Dulbecco's modified Eagle's medium, Ham's F-12 with 10% fetal bovine serum. Antipeptide antibodies recognizing Frmpd1 were generated by immunizing rabbits with the synthetic peptide CQHVIRMDQSPEEMQGAVRDTFQHLVQLAGL spanning amino acids 1473–1503 in human and 1444–1474 in rat and mouse. This sequence is identical in the three species with the exception of amino acids at the 2nd and 20th residue (2nd, Gln in rat and mouse, Arg in human; 20th, Asp in rat and mouse, Val in human). Peptides were synthesized by the Louisiana State University Health Sciences Center (LSUHSC) peptide synthesis facility and rabbits were immunized through the LSUHSC antibody production facility. Antiserum was characterized by analysis of varying amounts of GST-Frmpd1 fusion proteins and/or extracts from COS7 cells transfected with pcDNA3::Frmpd1 to determine optimal conditions for immunoblotting. The antiserum was affinity purified by the AminoLink Plus immobilization kit obtained from Pierce Chemical Company.

*Generation of Rat Frmpd1 Constructs*—Frmpd1 deletion constructs were generated by polymerase chain reaction from the Frmpd1 coding segment isolated in yeast two-hybrid screens and subcloned into pGEX4T1 for expression as GST fusion proteins. Primers were designed to add BamHI and XhoI sites to the 5′ and 3′ ends for GST-Frmpd1:Arg$^{871}$-Leu$^{1549}$ and GST-Frmpd1:Lys$^{1231}$-Leu$^{1549}$ and BamHI and SalI sites to the 5′ and 3′ ends for the rest of the GST-Frmpd1 constructs. Primers used to generate specific constructs are indicated below. All inserts were sequenced to verify fidelity: GST-Frmpd1 (Arg$^{871}$-Leu$^{1549}$), forward, 5′-CCCGGATCCAGAGAGCCCTACCTGAGCCTC and reverse, 5′-CCCCCGCTCGAGTCGACCTCACAGAGCGGTGGACGCCCGG; GST-Frmpd1 (Arg$^{871}$–Leu$^{1232}$), forward, 5′-CCCGGATCCAGAGAGCCCTACCTGAGCCTC and reverse, 5′-CCCGTCGACTCAAAGCTTTGGCAGGGGTGGTAC; GST-Frmpd1 (Lys$^{1231}$–Leu$^{1549}$), forward, 5′-CCCCGGATCCAAGCTTTCCCCGTGTCAAGAG and reverse, 5′-CCCCGCTCGAGTCGACCTCACAGAGCGGTGGACGCCCGG; GST-Frmpd1 (Arg$^{871}$–Glu$^{1051}$), forward, 5′-CCCGGATCCAGAGAGCCCTACCTGAGCCTC and reverse, 5′-CGCGTCGACTCATTCTGATCGCACTTCTTCCA; GST-Frmpd1 (Ser$^{1050}$–Leu$^{1549}$), forward, 5′-CGCGGATCCTCAGAAATGGGGTCAGGATCTGT and reverse, 5′-CGCGTCGACTCACAGAGCGGTGGACGCCCGG; GST-Frmpd1 (Ser$^{1050}$–Leu$^{1232}$), forward, 5′-CGCGGATCCTCAGAAATGGGGTCAGGATCTGT and reverse, 5′-CCCGTCGACTCAAAGCTTTGGCAGGGGTGGTAC; GST-Frmpd1 (Ala$^{901}$–Glu$^{1051}$), forward, 5′-CGCGGATCCGCCTTGGGGTTGCTGGCT and reverse, 5′-CGCGTCGACTCATTCTGATCGCACTTCTTCCA; GST-Frmpd1 (Ala$^{901}$–Pro$^{976}$), forward, 5′-CGCGGATCCGCCTTGGGGTTGCTGGCT and reverse, 5′-CGCGTCGACTCAGGGGTTGTGAGGGATGCTTGC; GST-Frmpd1 (His$^{977}$–Glu$^{1051}$), forward, 5′-CGCGGATCCCATCCTTCCAACCCAGGT and reverse, 5′-CGCGTCGACTCATTCTGATCGCACTTCTTCCA; GST-Frmpd1 (Ala$^{901}$–Val$^{938}$), forward, 5′-CGCGGATC**C**GCCTTGGGGTTGCTGGCT and reverse, 5′-CGCGTCGACTCACACTCGAGAGTCAATGACAGA; GST-Frmpd1 (Ser$^{939}$–Pro$^{976}$), forward, 5′-CGCGGATCCTCTTCTATCTCTGCCATTCGC and reverse, 5′-CGCGTCGACTCAGGGGTTGTGAGGGATGCTTGC.

*Generation of GST Fusion Proteins*—GST-tagged fusion proteins were expressed in BL-21 bacteria. Transformed bacteria were grown in 2× YT media (1.6% tryptone, 1% yeast extract, and 0.5% NaCl, pH 7.0) with 100 $\mu$g/ml ampicillin for 2 h at 37 °C and protein expression was then induced with isopropyl $\beta$-D-thiogalactopyranoside (100–300 $\mu$M) for 3 h at 30 °C. Induced cultures were centrifuged at 6,000 × *g* for 15 min at 4 °C. Bacterial pellets were resuspended using fusion protein buffer containing 140 mM NaCl, 10 mM $Na_2HPO_4$, 1.8 mM $KH_2PO_4$, 2.7 mM KCl, 1 mM dithiothreitol, 5 mM EDTA, and 5 mM EGTA with one protease inhibitor mixture tablet (Roche) per 10 ml of lysis buffer. The volume of fusion protein buffer

used was 12.5 ml/500 ml of bacteria culture. Lysates were sonicated and proteins solubilized by the addition of Triton X-100 (2% final concentration) with 30 min incubation before pelleting at 12,000 × *g* for 10 min at 4 °C. The supernatant was then combined with a glutathione affinity matrix (glutathione-Sepharose 4B) and incubated overnight at 4 °C. After incubation, the matrix was washed consecutively with fusion protein buffer containing 500 mM NaCl and 250 mM NaCl and GST-tagged fusion protein was eluted from the matrix by incubation with 10–50 mM reduced glutathione. The fusion protein was then desalted into 20 mM Tris (pH 7.4) and concentrated by centrifugation using a Centricon 30–100-kDa molecular mass cut-off filter (Millipore). The yield of fusion proteins varied depending on their size, solubility, and elution efficiency.

*Protein Interaction Assays*—Rat brain was homogenized in lysis buffer A (50 mM Tris-HCl, pH 8.0, 150 mM NaCl, 5 mM EDTA, 5 mM EGTA, and 1% Nonidet P-40, protease inhibitor mixture tablet (Roche Diagnostics), 3 ml of lysis buffer A/g of tissue). The tissue homogenate was centrifuged at 27,000 × *g* for 30 min after a 1-h incubation on ice. Supernatants were collected and spun at 100,000 × *g* for 1 h to generate a detergent-soluble fraction. One mg of rat brain lysate protein was precleared by incubation with 50 μl of glutathione-Sepharose 4B (prewashed with buffer A) at 25 °C for 30 min. Precleared lysates were incubated with 1 μM GST or GST fusion proteins overnight at 4 °C. Protein complexes were then captured by 40 μl of prewashed glutathione-Sepharose 4B for 1 h at 4 °C. Tubes were microcentrifuged (800 × *g* for 5 min) at room temperature and resins were washed three times with 500 μl of buffer A with intervening centrifugation. The proteins on the resin were resolved in protein sample buffer and the samples were then processed for SDS-PAGE and immunoblotting.

*Cell Transfection*—COS7 cells (80–90% confluent) in 100-mm plates were transfected with Lipofectamine 2000 in accordance with the manufacturer's instruction. Briefly, pcDNA3::Frmpd1 (10 μg) and pcDNA::AGS3 (3 μg) and/or pcDNA3::G$\alpha_{i3}$ (2 μg or 4 μg) in 500 μl of Opti-MEM media and 20 μl of Lipofectamine 2000 in 500 μl of Opti-MEM were mixed and then added to the cells in antibiotic-free growth media. The amount of DNA transfected was adjusted to 13 or 20 μg/plate in different experiments by adding pcDNA3 vector as necessary to maintain consistent plasmid load during transfection for appropriate sample comparison. The transfection mixture was removed 12 h later and replaced by normal growth medium and incubation was continued for 36 h. A series of preliminary experiments were conducted with a range of amounts of plasmid to optimize the expression level of the proteins and to identify any unexpected competition for expression that can occur with the transfection of multiple individual plasmid constructs.

For COS7 cells processed for fluorescent microscopy and immunocytochemistry, the following plasmids were transfected with Lipofectamine 2000 in accordance with the manufacturer's instruction: pEGFPN1 (0.2 μg), pmCherryN1 (0.2 μg), pmCherryN1::AGS3 (0.5 μg), pEGFPN1::AGS3 (0.5 μg), pEGFPN1::Frmpd1 (1.5 μg), pEGFPN1::Frmpd1 $Asn^{402}$–$Leu^{1578}$ (1.5 μg), and pcDNA3::G$\alpha_{i3}$ (0.3 μg). The amount of DNA transfected was adjusted to 2.0 μg/plate by adding pcDNA3 vector as necessary to maintain consistent plasmid load during transfection for appropriate sample comparison. Two μg of plasmid in 100 μl of Opti-MEM media and 4 μl of Lipofectamine 2000 in 100 μl of Opti-MEM were mixed and then added to the cells in antibiotic-free growth media. The cells were grown for an additional 48 h before processing for fluorescent microscopy or immunocytochemistry.

For Frmpd1 siRNA transfection in CAD cells, siRNA duplexes (siRNA number 1, nucleotides 1120–1144 5′-AGAAAGCCATTAGCTTCCACATGAA; siRNA number 2, nucleotides 1410–1434 5′-GAGTCTGAGAAAGTGAGCATGGTCA; siRNA number 3, nucleotides 2820–2844 5′-GAGATGGAGCCAGAGACCATGGAAA) targeted to the mouse Frmpd1 mRNA sequence (NM_001081172) were computationally identified as optimal sequences by Invitrogen. The conditions and duplex eliciting the most effective reduction in Frmpd1 were determined in a series of preliminary experiments. CAD cells at 60–70% confluence in 100-mm plates were transfected with a combination of Frmpd1 siRNA duplexes (nucleotides 1120–1144 and 1410–1434) using Lipofectamine 2000 according to the manufacturer's instructions. Briefly, RNA interference numbers 1 and 2 individually (80–120 nM) or in combination (80 nM each) in 400 μl of Dulbecco's modified Eagle's medium/F-12 media and 20 μl of Lipofectamine 2000 in 400 μl of Dulbecco's modified Eagle's medium were mixed and then added to the cells in antibiotic-free growth media. These conditions consistently reduced immunoreactive Frmpd1 by >80%. In control experiments, cells were transfected with the corresponding predicted oligonucleotide control for the Frmpd1 siRNA duplex: siRNA number 1, 5′-AGAACCGGATTCTTCACACTAAGAA, siRNA number 2, 5′-GAGGAGTGAAAGAGTGTACGCTTCA, or siRNA number 3, 5′-GAGAGGCCGAGACAGTACGGATAAA. The transfection mixture was removed 12 h later and replaced by normal growth medium with incubation continued for 36 h.

*Immunoprecipitation*—Transfected cells were lysed in 200–300 μl of buffer A. Lysates were precleared by incubation with 50 μl of GammaBind G-Sepharose (prewashed with buffer A) at 4 °C for 30 min. Precleared lysates (~800 μg of protein in 500 μl) were immunoprecipitated with affinity purified AGS3 PEP-32 antibody (6 μg/ml) at 4 °C overnight. Forty μl of 50% glutathione-Sepharose 4B (prewashed with lysis buffer A) were added and tubes rotated at 4 °C for another 40 min followed by centrifugation (800 × *g*, 4 °C, 5 min). Resins were washed 3 times with 500 μl of buffer A, with resin pelleting each time (800 × *g*, 4 °C, 5 min). The samples were then processed for SDS-PAGE and immunoblotting. Stripping and reprobing of membrane transfers with different antibodies was as previously described (6).

*Fluorescent Microscopy and Immunocytochemistry*—COS7 cells were seeded at 2 × $10^5$ cells/2 ml into six-well plates containing sterilized coverslips precoated with 0.01% polylysine and cells were grown to 80–90% confluence before transfection. Forty-eight h post-transfection, cells were washed twice with CWS (137 mM NaCl, 2.6 mM KCl, 1.8 mM $KH_2PO_4$, 10 mM $Na_2HPO_4$, pH 7.4) and fixed with 4% paraformaldehyde, 4% sucrose in CWS for 15 min and then rinsed twice with CWS. Cells were then stained with 4,6-diamidino-2-phenylindole for

5 min followed by a final wash with CWS for 15 min. Coverslips were mounted and fluorescence imaged with a Leica CTR5500 fluorescent microscope.

For cells processed for immunocytochemistry, cells were washed 3 times for 5 min with CWS after fixation and then permeabilized with 0.2% Triton X-100 in CWS for 5 min, followed by three 5-min CWS washes. 5% Normal donkey serum was used as a blocking agent for 1 h, followed by a 2-h incubation with primary antibody ($G\alpha_{i3}$ antiserum) diluted 1:200 in CWS and a 1-h incubation with secondary antibody (goat anti-rabbit Alexa Fluor 594, highly cross-adsorbed, Molecular Probes) diluted 1:2,000 in CWS. The antibody dilutions were centrifuged at 10,000 × *g* for 10 min prior to use. Cells were then stained with 4,6-diamidino-2-phenylindole and the coverslips were mounted as previously described. All images were obtained from approximately the middle plane of the cells.

*Measurement of Cyclic AMP*—CAD cells in 100-mm dishes were transfected with Frmpd1 siRNA or control siRNA as described above. 24 h post-transfection, CAD cells ($8\times10^4$) were replated onto 24-well plates and cultured for an additional 24 h followed by incubation for 1 h in 250 μl of serum-free media. Cells were then treated with 1 μM forskolin plus or minus UK-14304 (1 nM to 10 μM) in 50 μl of serum-free media containing 0.1 mM isobutylmethylxanthine for 5 min at 37 °C and 5% $CO_2$. The reactions were stopped by adding 33 μl of 10× lysis buffer provided by the cAMP Biotrak Enzyme Immunoassay kit manufacturer (Amersham Biosciences). Sample lysates were diluted 10 to 30-fold and 0.1 ml of diluted samples were transferred into a 96-well EIA plate. The cAMP levels were measured by measuring the absorbance values at 655 nm on a Model 680 Microplate Reader (Bio-Rad). The amount of cAMP in each well was determined by comparing the absorbance values of the treated variables with a series of standards. For each experiment the standards were assayed in parallel and used to generate a standard curve with a linear detection range that spanned 25–3200 fmol/well.

*Cell Fractionation*—100-mm dishes of COS7 or CAD cells were washed twice with CWS. Ninety percent of the cells were processed for fractionation and the remaining cells lysed by homogenization with a 26⅜-gauge syringe in Buffer A. Following a 1-h incubation on ice the latter aliquot of lysed cells were centrifuged at 100,000 × *g* to obtain a whole cell lysate. The major portion of the cells harvested for fractionation were homogenized in hypotonic lysis buffer (5 mM Tris-HCl, 5 mM EDTA, 5 mM EGTA, pH 7.4, and protease inhibitor mixture tablet) with a 26⅜-gauge syringe. The lysate were then centrifuged at 100,000 × *g* for 30 min at 4 °C to generate a membrane pellet and a 100,000 × *g* supernatant containing cytosol protein. In some experiments, lysed and homogenized cell extracts were fractionated following an initial centrifugation at 1,000 × *g* for 10 min to pellet any unlyzed cells and nuclei. The post-nuclear supernatants were then centrifuged at 100,000 × *g* for 30 min at 4 °C to generate a membrane pellet and a 100,000 × *g* supernatant containing cytosol protein. Both approaches yielded similar results in terms of the distribution of Frmpd1 and AGS3. Cell membrane pellets were washed by intervening homogenization in 500 μl of membrane buffer (50 mM Tris-HCl, pH 7.4, 0.6 mM EDTA, 5 mM $MgCl_2$ and protease inhibitor mixture tablet) or membrane buffer containing 100 mM NaCl and centrifuged at 100,000 × *g* for 30 min at 4 °C. The washed membrane pellets were resuspended in membrane buffer or lysis buffer A and directly processed for SDS-PAGE or resuspended in lysis buffer A followed by 100,000 × *g* centrifugation to generate a solubilized sample facilitating protein quantitation.

## RESULTS AND DISCUSSION

*Identification of AGS3 Binding Partners*—The subcellular distribution of AGS3-TPR ($Met^1$–$Pro^{463}$) is identical to that of full-length AGS3, which is nonhomogenously distributed within the cytosol and at regions of the plasma membrane suggesting that the TPR domains play an important role in cellular positioning of AGS3 (39). To identify candidate regulatory proteins that may be involved in this process, we conducted a series of yeast two-hybrid screens with the AGS3 TPR-linker region of AGS3 ($Met^1$–$Pro^{463}$). Yeast two-hybrid screens of a rat brain library and a mouse 11-day-old embryonic with AGS3-TPR identified five candidate AGS3 binding partners: MACF (AAD32244), ROBO-1 (NP_062286), LKB1 (NP_035622), MARCKS-like protein (CAM17499), and KIAA0967 (Frmpd1) (XP_233002) (35). Seven of the cDNAs identified in the yeast two-hybrid screen encoded different amino-terminal truncated regions in the carboxyl terminus (CT) ($Arg^{871}$–$Leu^{1549}$) of Frmpd1.[3] Rat Frmpd1 (XP_233002) is a predicted protein (~169 kDa) encoded by a predicted mRNA of 4912 nucleotides, which contains one PDZ (Postsynaptic density protein-95, Discs large, Zonula occludens-1) ($Gln^{67}$–$Thr^{135}$) and one Band 4.1 or FERM domain (Band *4*.1, ezrin/radixin/moesin protein domain) ($Leu^{177}$–$Phe^{401}$) (Fig. 1). There are no readily identifiable domains in the remainder of the protein. Rat Frmpd1 exhibits 89 and 74% amino acid sequence identity with mouse (NP_001074641) and human Frmpd1 (NP_055722, BAA76811), respectively.[4] Messenger RNA blots, reverse transcriptase-PCR, and immunoblot data indicate expression of Frmpd1 in several tissues and cell lines that similarly express AGS3 (*i.e.* rat testis (7), rat brain (6, 7), mouse catecholaminergic cell line Cath.a-differentiated (CAD) neuronal cells, neuroblastoma-glioma hybrid cell line NG108-15 (6), rat pheochromocytoma neuron-like cell line PC-12 (6), rat testis teratocarcinoma cell line F9, and low or undetectable levels in the mouse Leydig cell line TM3) (supplemental Fig. S1, see also Fig. 5).[5]

The general organization and positioning of the PDZ and FERM domains in Frmpd1 is also found in Frmpd3 (KIAA1817, Q5JV73, PDZ domain containing 10) and Frmpd4 (KIAA0316, BAA20774) (supplemental Fig. S2) as determined with the Simple Modular Architecture Research

[3] The cDNAs encoding regions of KIAA0967 were not in-frame with the GAL4 activation domain consistent with known flexibility of yeast translation mechanisms in such screens.

[4] CRA_a (EAW58271) encodes a predicted protein that differs from the protein encoded by human Frmpd1 mRNA (BAA76811) by one amino acid ($Ser^{1278}$ instead of $Leu^{1278}$) that results from a 1-nucleotide difference in the gene and mRNA. It is not clear if this is due to a sequencing error, mRNA editing, or if it represents a polymorphism in the gene.

[5] N. An and S. M. Lanier, unpublished observations.

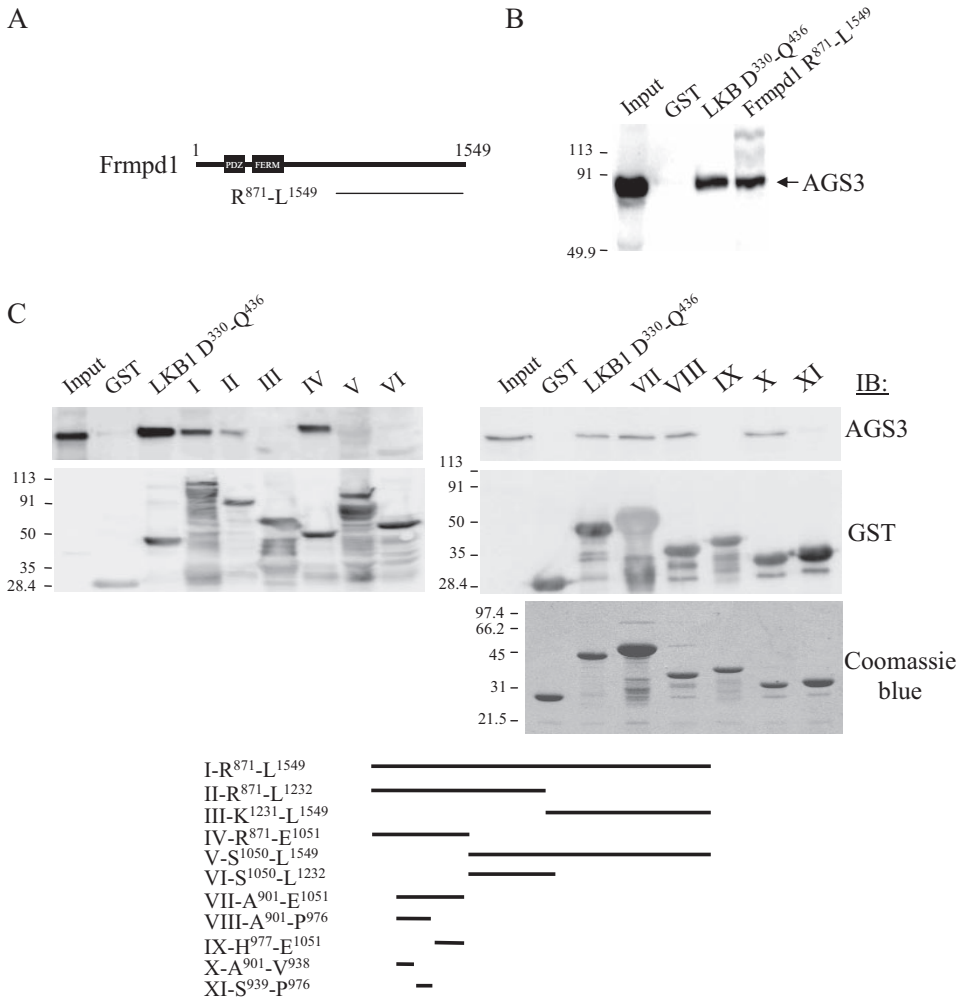


FIGURE 1. **Interaction of Frmpd1 and AGS3 *in vitro*.** *A*, schematic diagram of Frmpd1 indicating the location and length of the Frmpd1 fragment ($Arg^{871}$–$Leu^{1549}$) isolated in the yeast two-hybrid screen. *B*, rat brain lysate (1 mg of protein) was incubated with 1 $\mu$M GST, GST-LKB1-CT ($Asp^{330}$–$Gln^{436}$), or GST-Frmpd1 ($Arg^{871}$–$Leu^{1549}$) for 1 h at 24 °C and processed by GST pull-down assays, SDS-PAGE, and immunoblotting as described under "Experimental Procedures." Membrane transfers were first probed with affinity purified AGS3 antibody (PEP32 0.22 $\mu$g/ml, *left panel*). The *Input* lane contains 1/10 of the lysate volume used for each interaction assay. Data represent at least four independent experiments. *C*, the continually truncated GST-Frmpd1 proteins (1 $\mu$M) were incubated with rat brain lysate and processed with GST pull-down assays as described for *panel B*. The *two upper blots* in *C* were stripped and reprobed with GST antibody (*middle panels*) to verify protein loading. A Coomassie Blue stain of the GST fusion proteins was included to indicate the quality of the preparation (*lower right panel*). The location and length of truncated Frmpd1 deletion constructs are indicated in the *lower panel*. Data shown are representative of at least three independent experiments with similar results using different brain lysates and/or fusion protein preparations.

Tool (SMART) (56). Human Frmpd1 exhibits 19 and 21% overall amino acid identity to Frmpd3 and Frmpd4, respectively. Human Frmpd3 and Frmpd4 exhibit 24% overall amino acid identity with each other. The amino-terminal ~500 amino acids containing the PDZ and FERM domains in Frmpd1 exhibit 33 and 41% amino acid identity with Frmpd3 and Frmpd4, respectively, whereas Frmpd3 and Frmpd4 exhibit 44% homology in this region.

Frmpd2 (NP_689641) is more representative of a separate group of proteins with PDZ and FERM domains that differ from group I by the number and position of the PDZ domain(s) (supplemental Fig. 2). Frmpd2 contains a KIND (kinase non-catalytic C-lobe domain) at the amino-terminal and three PDZ domains downstream of the FERM domain. A similar domain organization is found in tyrosine-protein phosphatase non-receptor type 13 (protein-tyrosine phosphatase 1E (UPI000000457247, similar to Q12923). This protein contains five PDZ domains downstream of the FERM domain and a protein-tyrosine phosphatase, catalytic domain at the carboxyl-terminal of the protein. A third group of proteins with FERM and PDZ domains include the protein-tyrosine phosphatase non-receptor types 3 (Q45VJ3) and 4 (P29074). This group of proteins is characterized by the presence of one PDZ domain downstream of a FERM domain with a protein-tyrosine phosphatase, catalytic domain motif at the carboxyl-terminal of the protein (supplemental Fig. S2).

The function of Frmpd1 is not known and the gene was only recently named. Proteins with a somewhat similar domain organization are found in *Caenorhabditis elegans* (Q8MXF0, Frm-8) and *Drosophila melanogaster* (Q9VFD3), but none of these related proteins are functionally defined. One of the key questions for AGS3 and other GPR-containing proteins is what regulates their subcellular location and interaction with G-proteins. Frmpd1 is particularly interesting in this context as PDZ and FERM domains are implicated in docking of proteins within larger signaling complexes and in linkages between the cytoskeleton and plasma membrane (43–47).

*Interaction of AGS3 and Frmpd1*—The interaction of Frmpd1 and AGS3 identified in the yeast two-hybrid screen was first validated by GST pull down and coimmunoprecipitation experiments. Rat Frmpd1-CT ($Arg^{871}$–$Leu^{1549}$) effectively interacted with AGS3 in rat brain lysates (Fig. 1*B*). The AGS3 binding partner LKB1-CT ($Asp^{330}$–$Gln^{436}$) served as a positive internal control (35). Subsequent deletion mutagenesis localized the AGS3 binding domain of Frmpd1 to a 38-amino acid peptide ($Ala^{901}$–$Val^{938}$) (Fig. 1*C*).[6]

Due to the challenge of generating intact, pure preparations of such large proteins, the sensitivity of the larger GST-Frmpd1

[6] The additional immunoreactive species observed with the GST immunoblot after incubation with brain cytosol *versus* the Coomassie Blue-stained purified proteins (Fig. 1*C*) represents both the sensitivity of the antibody and any cross-reactive cytosolic proteins retained by the glutathione beads upon pull down.

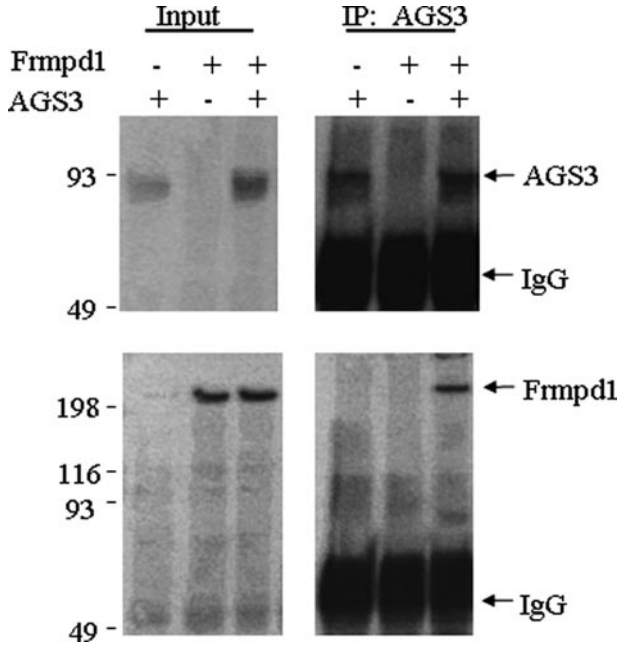


FIGURE 2. **Coimmunoprecipitation of Frmpd1 and AGS3 from COS-7 cell lysates.** COS-7 cells were transfected, harvested, and processed for immunoprecipitation as described under "Experimental Procedures." Precleared lysates (800 $\mu$g of protein in 500 $\mu$l total volume) were immunoprecipitated with affinity purified AGS3 antibody (PEP32) and processed for SDS-PAGE and immunoblotting. The *Input* lanes represent 1/15 of the lysate volume used for immunoprecipitation. The blot was probed with Frmpd1 antibody (0.4 $\mu$g/ml) and AGS3 antibody (PEP32, 0.22 $\mu$g/ml). The data presented are representative of at least four independent experiments. *IP*, immunoprecipitation.

fusion proteins to proteolysis and to move forward with cell-based studies, the interaction between full-length Frmpd1 and AGS3 was characterized in the intact cell. COS7 cells transfected with pcDNA3::Frmpd1 expressed a specific immunoreactive species detected by the Frmpd1 antibody with a molecular mass of ~200 kDa (Fig. 2).[7] In cells co-transfected with pcDNA3::AGS3 and pcDNA3::Frmpd1, Frmpd1 co-immunoprecipitated with AGS3 (Fig. 2).[8] Thus, the interaction of AGS3 with the fragment of Frmpd1 first identified in the yeast two-hybrid screen was validated in GST-pull down assays and by coimmunoprecipitation of AGS3 with intact, full-length Frmpd1 from cell lysates. We then asked if this interaction influenced the positioning of AGS3 within the cell and/or its ability to bind $G\alpha_i$.

*Influence of Frmpd1 on the Subcellular Positioning of AGS3*—AGS3 exhibits primarily a nonhomogeneous distribution in the cytosol as previously reported for transfected and endogenous AGS3 with some pockets of apparent membrane association (6, 7, 18, 32, 39). However, $G\alpha_{i3}$ is predominately at the plasma membrane and in the Golgi apparatus and endoplasmic reticulum (18, 25, 48–51). Several observations indicate that the subcellular location of AGS3 and its interaction with G-proteins are regulated events. First, a subpopulation of AGS3 and $G\alpha_i$ are complexed with each other within the cell even though AGS3 is enriched in the 100,000 × *g* supernatant and $G\alpha_{i3}$ is enriched in the 100,000 × *g* pellet following non-detergent, hypotonic lysis of cells or tissues (6, 39). The AGS3 found in the 100,000 × *g* pellet is loosely associated and can be decreased with repeated washings of the pellet, whereas this is not the case for $G\alpha_{i3}$. Second, removal of the TPR domains from AGS3 as observed with AGS3-SHORT, which contains three GPR motifs, results in a protein that can easily be redirected to the plasma membrane from the cytosol by simply increasing the levels of $G\alpha_{i3}$ (39). Immunofluorescent imaging indicates that increased expression of $G\alpha_{i3}$ or $G\alpha_o$ also readily increases the amount of the AGS3-related protein AGS5/LGN at the cell periphery (17, 25, 26). This effect of increased levels of $G\alpha_{i3}$ is not observed with AGS3-SHORT Q/A or the AGS5/LGN Q/A mutant, which contains a mutation in each of the GPR motifs that eliminates $G\alpha_i$ binding (25, 52).[9] Third, AGS3 and AGS5/LGN exhibit different distribution profiles following sucrose gradient fractionation of neuronal lysates (29). Fourth, both AGS3 or AGS5/LGN and $G\alpha_{i3}$ are present at the spindle pole during cell division (25, 51). These data suggest that the subcellular location of AGS3 and its interaction with G-proteins is a regulated event.

Both PDZ and FERM domains are associated with the positioning of proteins at the interface of the cytoskeleton network and the membrane (43–47). In COS7 cells, transfected AGS3 is primarily found in the 100,000 × *g* supernatant following hypotonic lysis with a fraction in the membrane pellet (Fig. 3*A*). Frmpd1 distributed to both the 100,000 × *g* supernatant and pellet. Distribution of Frmpd1 to the membrane pellet required the presence of the FERM domain (supplemental Fig. S3). As AGS3 interacts with the carboxyl terminal of Frmpd1, the PDZ and FERM domains may be free to interact with other binding partners that would influence the subcellular trafficking of AGS3. Indeed, in COS7 cells transfected with pcDNA3::AGS3, Frmpd1 stabilized the fraction of AGS3 associated with the 100,000 × *g* pellet (Fig. 3). The amount of AGS3 in the 100,000 × *g* pellet was increased by ~2-fold when cells were cotransfected with Frmpd1, whereas the amount of AGS3 in the 100,000 × *g* supernatant was unaltered (Fig. 3*C*). This increase appears to reflect a stabilization of AGS3 in a membrane fraction as indicated by the resistance of membrane-associated AGS3 to membrane pellet washing observed in the presence of Frmpd1 (Fig. 3*B*).[10] The increase in membrane-associated AGS3 observed in the presence of Frmpd1 likely reflects both retention of AGS3 that is lost during pellet washing and the preferred positioning of AGS3 in a membrane fraction when complexed with Frmpd1. The relative distribution of Frmpd1 in the pellet and supernatant was not altered by overexpression of AGS3 (Fig. 3*C*).

The influence of Frmpd1 on the subcellular positioning of AGS3 was further addressed by fluorescent imaging using

[7] The molecular mass of ~200 kDa is greater than the calculated molecular mass of 173.4 and this may relate to the proline content (7.4%) of Frmpd1 and/or its acidic pI.

[8] Comparative immunoblot analysis of transfected cell lysates and GST-AGS3 ($Pro^{463}$–$Ser^{650}$, molecular mass ~50 kDa) or GST-Frmpd1 (GST Fr, $Lys^{1231}$–$Leu^{1549}$, molecular mass ~60 kDa) indicated similar expression levels of Frmpd1 and AGS3 (~60–100 pmol/mg of cellular protein).

[9] J. B. Blumer, V. Simon, N. An, and S. M. Lanier, unpublished observations.

[10] Similar results were obtained using wash buffer containing 100 mM NaCl.

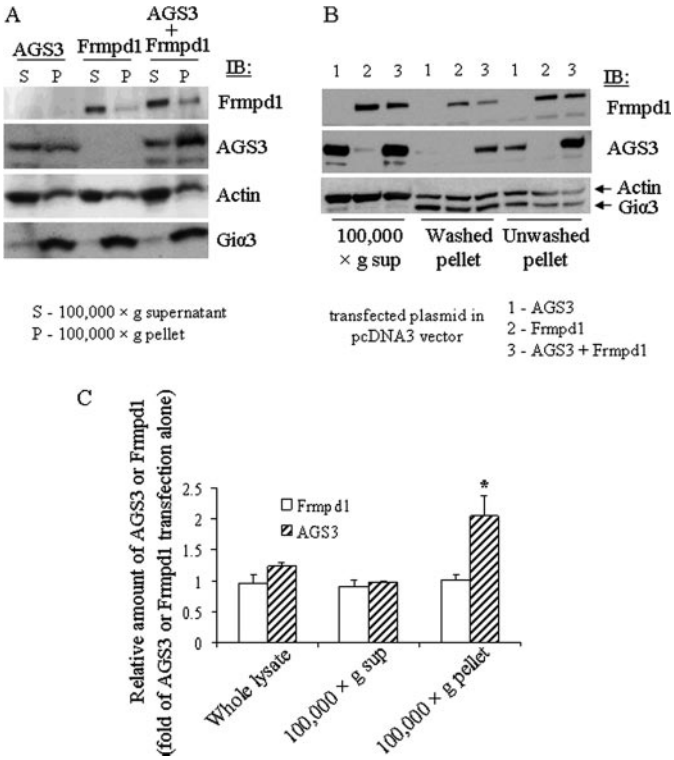


FIGURE 3. **Influence of Frmpd1 on fractionation of AGS3.** *A*, COS7 cells were transfected with pcDNA3::Frmpd1, pcDNA3::AGS3, or co-transfected with both constructs, lysed, and processed for fractionation as described under "Experimental Procedures." Forty $\mu$g of cytosol protein (100,000 $\times$ *g* supernatant) and 60 $\mu$g of washed membrane protein (100,000 $\times$ *g* pellet, washed with membrane buffer: 50 mM Tris-HCl, pH 7.4, 0.6 mM EDTA, 5 mM $MgCl_2$) were then processed for SDS-PAGE and immunoblotting. Data represent at least eight independent experiments. *B*, COS7 cells were transfected as described in *A* and fractionated as described under "Experimental Procedures" to generate a washed and unwashed membrane pellet. Sixty $\mu$g of cytosol proteins, 54 $\mu$g of washed membrane proteins, and 60 $\mu$g of unwashed membrane proteins were processed for SDS-PAGE and immunoblotting. *C*, data are presented in the *bar graph* as the mean $\pm$ S.E. (whole cell lysate: AGS3, $n = 3$; Frmpd1, $n = 2$; 100,000 $\times$ *g* supernatant and pellet: AGS3, $n = 8$; Frmpd1, $n = 6$). The pixel intensity of AGS3 or Frmpd1 in each fraction observed when cells were cotransfected was divided by the pixel intensity of the corresponding immunoreactive species observed in that specific fraction when cells were transfected with AGS3 or Frmpd1 alone and normalized according to actin expression level. Statistical significance was evaluated with the Student's *t* test (*, $p < 0.05$). The following antibodies were used: Frmpd1 (0.4 $\mu$g/ml), AGS3 (PEP32, 0.22 $\mu$g/ml), $G\alpha_{i3}$ antisera (1:2,000), and actin (0.5 $\mu$g/ml).

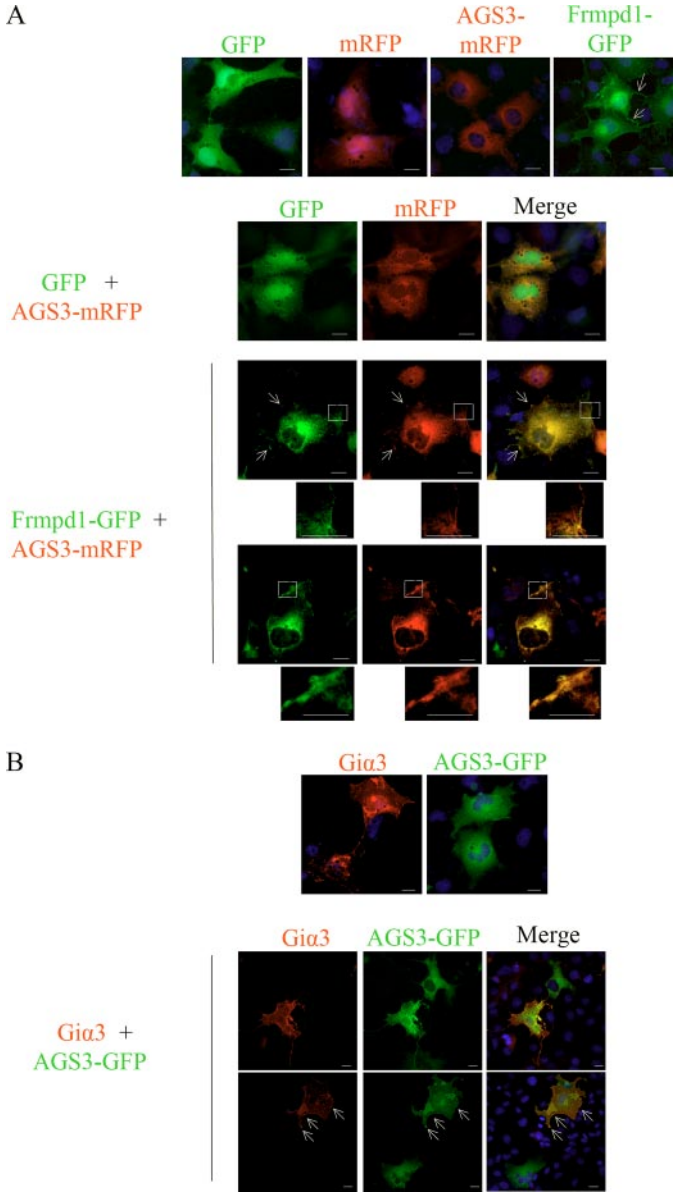


FIGURE 4. **Influence of Frmpd1 on subcellular localization of AGS3.** *A*, COS7 cells (80–90% confluence) were transfected with plasmids as indicated and processed for fluorescence microscopy as described under "Experimental Procedures." DNA was stained by 4,6-diamidino-2-phenylindole (*DAPI*) (1 $\mu$g/ml) (*blue*). The *white arrows* point to the cell periphery. Images were taken from approximately the middle plane of the cell and are presented at $\times$63 magnification. The enlarged images are defined by the *dashed inset* demonstrating co-localization of AGS3-mRFP and Frmpd1-GFP at the cell periphery. Data are representative of three independent experiments. *B*, COS7 cells transfected with pEGFPN1::AGS3, pcDNA3::$G\alpha_{i3}$ or both constructs were processed for immunocytochemistry as described under "Experimental Procedures." The patch with enhanced GFP background fluorescence reflects a section of the cell that folded back on itself during preparation. The images shown are representative of at least four independent experiments. *Scale bar*, 10 $\mu$m.

pEGFPN1::Frmpd1 and pmCherryN1::AGS3. In the absence of Frmpd1-GFP, AGS3-mRFP is primarily localized in the cytosol with some apparent membrane association as previously reported (6, 7, 18, 32, 39). Frmpd1-GFP is also predominantly nonhomogeneously distributed in the cytosol but is also found at the cell cortex membrane and in processes similar to membrane ruffles or microspikes.[11] As is commonly the case with transfected proteins, both AGS3 and Frmpd1 are also distributed in subcellular organelles associated with various aspects of protein translation that likely accounts for some of the signal overlap within the cell. The distribution of Frmpd1-GFP in the cell cortex or membrane structures requires the presence of the PDZ and FERM domains as the amino-terminal deletion construct of human Frmpd1 ($Asn^{402}$–$Leu^{1578}$–GFP), which lacks the PDZ and FERM domains, exhibits a diffuse cytoslic distribution (supplemental Fig. S3 and 4). These data parallel the differences in subcellular distribution observed for the two constructs upon immunoblotting of the 100,000 $\times$ *g* supernatant and 100,000 $\times$ *g* pellet (supplemental Fig. S3).

[11] Cells expressing Frmpd1 generally exhibited a more defined set of extracellular processes that may relate to the required role of FERM domains themselves when found in proteins associated with the promotion of membrane extensions (54, 55).

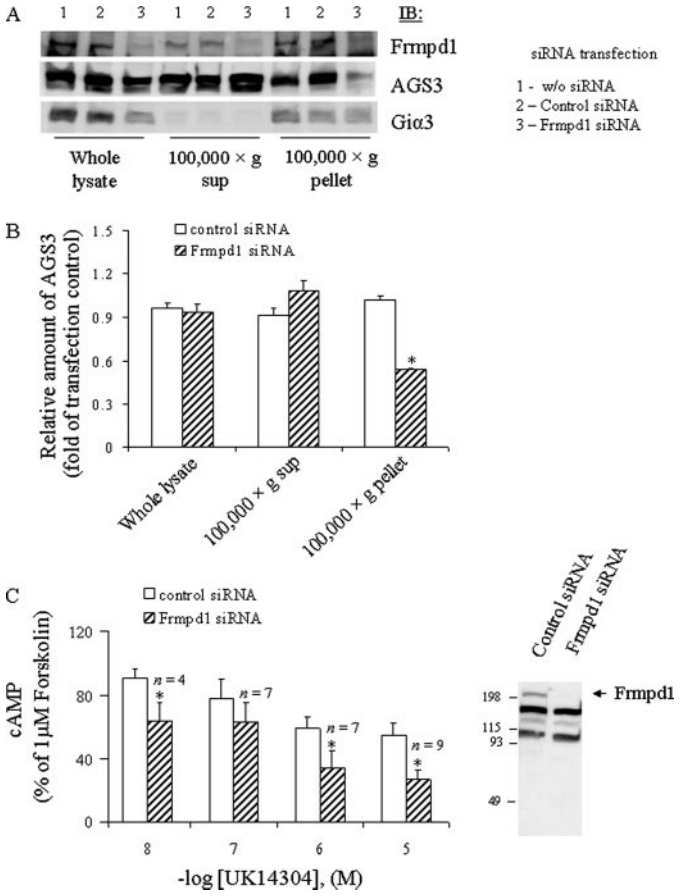


FIGURE 5. **Influence of siRNA-mediated knockdown of Frmpd1 on fractionation of AGS3 and receptor-mediated regulation of cAMP in CAD cells.** *A*, CAD cells (60–70% confluence in 100-mm dish) were transfected with 80 nM Frmpd1 siRNA number 1 plus 80 nM Frmpd1 siRNA number 2 and processed for fractionation as described under "Experimental Procedures." Forty $\mu$g of whole lysate protein and cytosol protein or 100 $\mu$g of membrane protein were electrophoresed and membrane transfers were probed with Frmpd1 antibody (0.4 $\mu$g/ml), AGS3 antibody (PEP32, 0.22 $\mu$g/ml), and G$\alpha_{i3}$ antisera (1:2,000). *B*, data are presented in the *bar graph* as the mean ± S.E. ($n = 4$). The pixel intensity of AGS3 or Frmpd1 in each fraction observed following siRNA-mediated knockdown of Frmpd1 was divided by the pixel intensity of the corresponding immunoreactive species observed in that specific fraction when cells were transfected with control siRNA duplexes and normalized according to actin expression level. The transfection control refers to cells treated with transfection reagent but without siRNA. *C*, CAD cells were transfected with control siRNA or Frmpd1 siRNA as described above for *A*. 24 h post-transfection, the cells were replated on 24-well plates and treated with 1 $\mu$M forskolin plus or minus the $\alpha_2$-adrenergic receptor selective agonist UK-14304 (10 nM to 10 $\mu$M). Total cellular cAMP was measured as described under "Experimental Procedures." Basal cAMP: control siRNA, 5.75 ± 0.86 pmol/well, $n = 9$; Frmpd1 siRNA, 5.71 ± 0.77 pmol/well, $n = 9$. Forskolin-induced cAMP: control siRNA, 24.12 ± 3.59 pmol/well, $n = 9$; Frmpd1 siRNA, 21.16 ± 2.46 pmol/well, $n = 9$. The *right panel* indicates knockdown of Frmpd1 following Frmpd1 siRNA transfection from a representative experiment. Data are presented as the mean ± S.E. Statistical significance was evaluated with the Student's *t* test (*, $p < 0.05$); *n*, number of independent experiments.

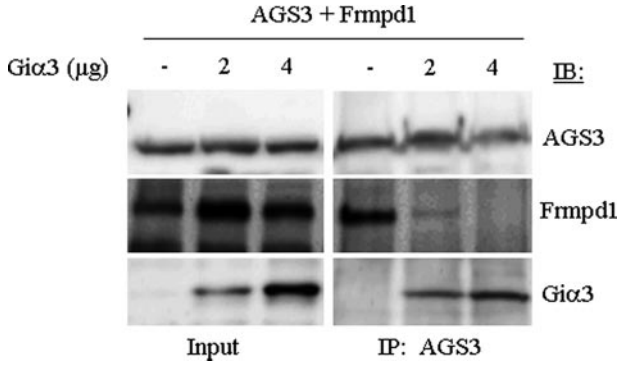


FIGURE 6. **Interaction of Frmpd1 and G$\alpha_{i3}$ with AGS3 in COS7 cells.** *A*, COS-7 cells were transfected with pcDNA3::Frmpd1 (10 $\mu$g) and pcDNA3::AGS3 (3 $\mu$g) or cotransfected with pcDNA3::Giα3 (2 or 4 $\mu$g). Cell lysates were prepared and processed for immunoprecipitation as described under "Experimental Procedures." Precleared lysates (800 $\mu$g of protein in 500 $\mu$l total volume) were immunoprecipitated (*IP*) with AGS3 antibody (PEP32) and processed for SDS-PAGE and immunoblotting (*IB*). Membrane transfers were probed with Frmpd1 antibody (0.4 $\mu$g/ml), AGS3 antibody (PEP32, 0.22 $\mu$g/ml), and G$\alpha_{i3}$ antisera (1:2,000). Data are representative of three experiments using different transfected cell lysates.

Upon cotransfection of pEGFPN1::Frmpd1 and pmCherryN1::AGS3, AGS3-mRFP is observed in regions of the cell cortex and also in membrane extensions or processes where it appears to be colocalized with Frmpd1-GFP based upon the merged fluorescent signals (Fig. 4*A*). The movement of AGS3 to regions at the cell cortex or at membrane extensions observed in the presence of Frmpd1 requires the PDZ and FERM domains to apparently provide a membrane anchor as this effect was not observed in Frmpd1 constructs lacking the PDZ and FERM domains (supplemental Fig. S4). As expected from GST-Frmpd1 pull down assays using different regions of Frmpd1, the PDZ and FERM domains are not required for interaction with AGS3 as Frmpd1 ($Asn^{402}$-$Leu^{1578}$)-GFP co-immunoprecipitates with AGS3 from COS7 cell lysates (supplemental Fig. S4).

$G_{i/o}$ protein also regulates the fractionation or subcellular localization of GPR proteins (17, 25, 39) upon transfection. We thus evaluated the influence of $Ga_{i3}$ on AGS3-GFP subcellular localization in COS7 cells by immunocytochemistry. G-protein is enriched at the cell cortex, whereas AGS3-GFP is predominantly found in the cytoplasm. Upon transfection with $Ga_{i3}$, portions of AGS3-GFP were present in cell extensions and at the cell cortex as readily observed by comparison with a cell in the same field that was only transfected with AGS3-GFP (Fig. 4*B*).

The regulation of AGS3 distribution by Frmpd1 was then addressed with cells expressing the endogenous proteins. CAD cells are one of several neuronal cell lines expressing both Frmpd1 and AGS3. Endogenous AGS3 was found in both the 100,000 × *g* pellet and supernatant (Fig. 5) as was Frmpd1. A series of siRNA oligonucleotides were designed and tested for their ability to reduce the levels of Frmpd1 in CAD cells. A major immunoactive band around 200 kDa was present in CAD cells, which is the same size as transfected human Frmpd1. Two of the three siRNA oligonucleotides effectively reduced the Frmpd1 protein by >80% (Fig. 5*A*, and supplemental Fig. S5). The siRNA-mediated knockdown of Frmpd1 did not influence the levels of total AGS3 expressed; however, it markedly reduced the amount of AGS3 found in the 100,000 × *g* pellet (Fig. 5, *A* and *B*).

These data with both transfected systems and siRNA-mediated reduction of endogenous Frmpd1 in cells also expressing AGS3 indicate that Frmpd1 plays an important role in positioning AGS3 within the cell by stabilizing the population of the protein in the membrane fraction. This is of particular note as such regulation may provide a mechanism to increase the population of AGS3 in a compartment

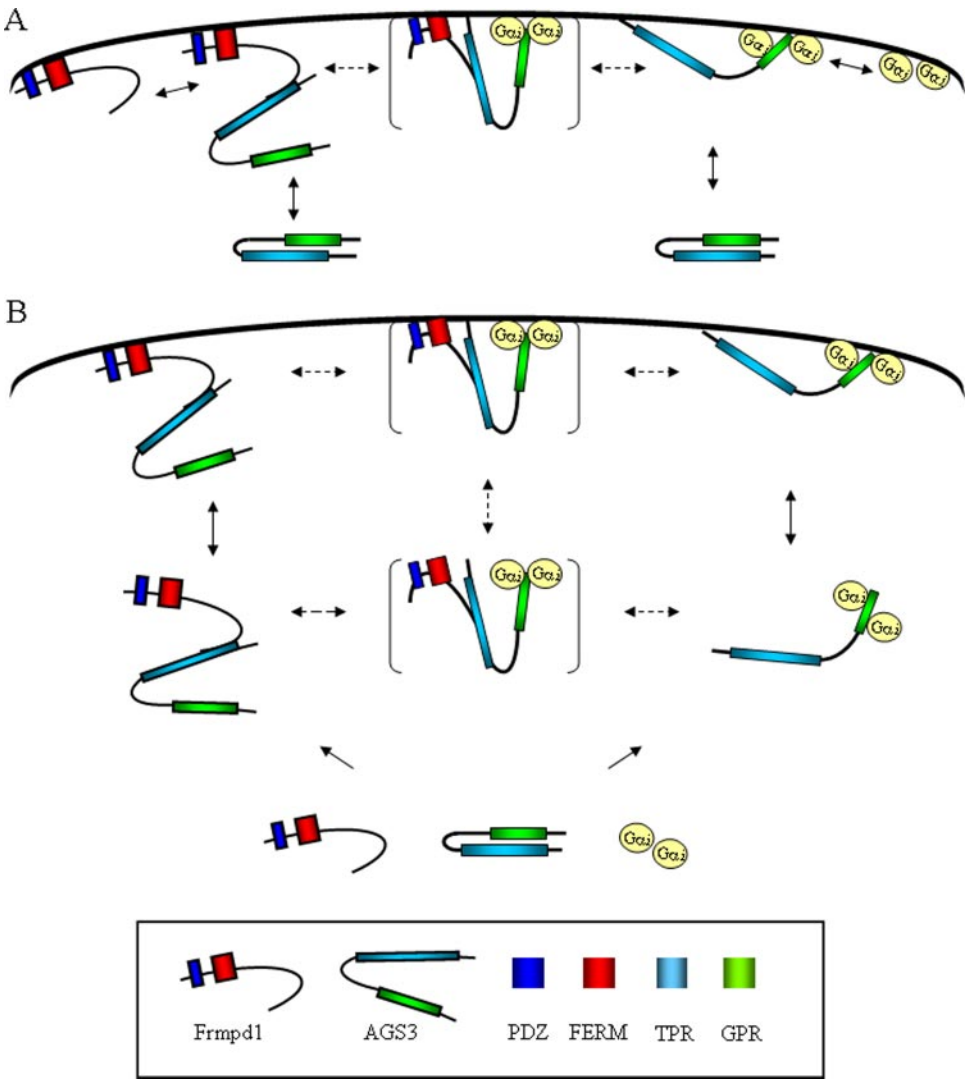


FIGURE 7. **Schematic representation of AGS3 positioning within the cell.** AGS3 may find its binding partners already positioned at the cell cortex (*A*) or it may find them in another subcellular compartment (*B*) and the complex would then move to the cell cortex. The *bracketed* entity and *dashed arrows* illustrate a postulated transient ternary complex. Up to four $G\alpha_i$ subunits may be docked to AGS3 (6, 53) and only two $G\alpha_i$ subunits are indicated in the schematic for the AGS3-$G\alpha_i$ complex simply for ease of presentation. Refer to "Results and Discussion" for further discussion.

enriched in G-proteins and/or influence the interaction of AGS3 with G-proteins.

*Influence of Frmpd1 Knockdown on Receptor-mediated Regulation of cAMP in CAD Cells*—As an initial approach to address the role of Frmpd1 in cell signaling, we examined the effect of Frmpd1 knockdown on the GPCR-mediated inhibition of adenylyl cyclase. Frmpd1 knockdown did not influence basal or forskolin-induced increases in cAMP. However, the $\alpha_2$-adrenergic receptor-mediated inhibition of forskolin-induced increases in cAMP was enhanced following Frmpd1 knockdown (Fig. 5*C*). Thus, the "positioning" of AGS3 within the cell is important relative to its ability to influence G-protein signaling.

*The Interaction of AGS3 with Frmpd1 and $G\alpha_{i3}$*—A subpopulation of AGS3 and $G\alpha_i$ apparently exists bound to each other in tissue and cell lysates and up to four $G\alpha_i$ molecules may be complexed with AGS3 at any given moment (6, 53). The interaction of AGS3 and other GPR proteins with $G\alpha_i$ or $G\alpha_o$ is likely regulated as described above, but we do not as yet fully understand the mechanisms by which this regulation is achieved both with respect to association and dissociation. AGS5/LGN and the *D. melanogaster* AGS3/AGS5 ortholog PINS both have TPR/linker binding partners that influence their subcellular location (*i.e.*, NuMA-AGS5/LGN (15, 26), Insc-AGS5/LGN or PINS (19–21, 34), Dlg-PINS (13, 30), Lgl2-AGS5/LGN (38), and Mud-PINS (36, 37)). In each case, the interaction of the binding partner either facilitates or does not alter their interaction with $G\alpha_i$. AGS5/LGN also interacts with SAP102 and PSD-95, which is important for its location within neuronal extensions and the regulation of *N*-methyl-D-asparatate receptor trafficking (29); interestingly, $G\alpha$ is part of this complex (29). The mammalian ortholog of inscuteable (mInsc) also binds to AGS3, however, the consequences of this interaction and whether G-protein is part of this complex is not known (34). The AGS3-TPR domain binds the serine/threonine kinase LKB1, which is postulated to phosphorylate residues in the GPR domains that may influence G-protein interaction (35).

As a first approach to determine the dynamics of the interaction of AGS3, Frmpd1, and $G\alpha_i$, we asked if Frmpd1 and $G\alpha_{i3}$ could simultaneously bind to AGS3. COS7 cells were transfected with pcDNA3::AGS3 and pcDNA3::Frmpd1 without and with increasing amounts of pcDNA3::$G\alpha_{i3}$. The level of $G\alpha_{i3}$ protein expressed was related to the amount of pcDNA3::$G\alpha_{i3}$ used for transfection (Fig. 6). In the absence of transfected $G\alpha_{i3}$, AGS3 and Frmpd1 co-immunoprecipitate as in Fig. 2. However, this interaction is lost as the amount of $G\alpha_{i3}$ in the cell is increased and AGS3 apparently switches its binding partner from Frmpd1 to $G\alpha_{i3}$ (Fig. 6). These data suggest that the interaction of AGS3 with Frmpd1 and $G\alpha_{i3}$ is mutually exclusive.

The interaction of AGS3 with its different binding partners and its positioning within the cell is illustrated in Fig. 7. AGS3 in the cytosol may position itself at the cell cortex via interaction with membrane-bound Frmpd1 or membrane-bound G-protein (Fig. 7*A*). AGS3 may also find its binding partners (Frmpd1 or $G\alpha_i$) in another cellular compartment and the AGS3-Frmpd1 or AGS3-$G\alpha_i$ complexes would then traffic to the cell cortex (Fig. 7*B*). Alternatively, a transient ternary complex

(*bracketed* entity in Fig. 7) of Frmpd1-AGS3-G$\alpha_i$ is formed in the cytosol, which then traffics to the cell cortex where it destabilizes to either a Frmpd1-AGS3 or G$\alpha_i$-AGS3 complex. The postulated existence of such a ternary complex would also allow AGS3 to switch its binding partners once it is positioned at the cell cortex. The stabilization and destabilization of the postulated ternary complex may be regulated by other factors such as lipids or other binding partners.

The regulatory interaction of Frmpd1 with AGS3 and G$\alpha$ described herein thus differs from that observed for the interaction of Insc or NuMA/Mud, SAP102 or PSD95 with AGS5/LGN or the *D. melanogaster* AGS3/AGS5 ortholog PINS and G$\alpha$. In each case, the GPR protein is apparently complexed with both its TPR binding partner and G$\alpha$. As Frmpd1 and G$\alpha_{i3}$ interact with distinct regions of AGS3, the mutually exclusive interaction of these two proteins with AGS3 is not likely due to competition for shared binding sites. The conformation of AGS3 when it is complexed with G$\alpha_{i3}$ may result in a rearrangement of the Frmpd1 binding site on AGS3 or simply render it inaccessible. Alternatively, interaction of AGS3 with Frmpd1 or G$\alpha_{i3}$ may differentially restrict the distribution of AGS3 within membrane compartments such that is does not have access to both binding partners. Our data suggest that the interaction of AGS3 with Frmpd1 facilitates membrane recruitment of AGS3 where Frmpd1 can be exchanged for G$\alpha_i$ in a regulated manner.

*Acknowledgments—We very much appreciate the technical assistance provided by Maureen Fallon, Peter Chung, and Shilpa A. Yelundur as well as the assistance provided by Joseph Chaiban with antibody production. S. M. L. is very grateful to Professors Claude Bouchard and Thomas W. Gettys, Pennington Biomedical Research Center, Baton Rouge, LA, and Dr. Seth Pincus, The Research Institute for Children (Children's Hospital, New Orleans, LA), for providing laboratory and office space after Hurricane Katrina.*

## REFERENCES

1. Blumer, J. B., Smrcka, A. V., and Lanier, S. M. (2007) *Pharmacol. Ther.* **113,** 488–506
2. Sato, M., Blumer, J. B., Simon, V., and Lanier, S. M. (2006) *Annu. Rev. Pharmacol. Toxicol.* **46,** 151–187
3. Cismowski, M. J., and Lanier, S. M. (2005) *Rev. Physiol. Biochem. Pharmacol.* **155,** 57–80
4. Cismowski, M. J., Takesono, A., Ma, C., Lizano, J. S., Xie, X., Fuernkranz, H., Lanier, S. M., and Duzic, E. (1999) *Nat. Biotechnol.* **17,** 878–883
5. Takesono, A., Cismowski, M. J., Ribas, C., Bernard, M., Chung, P., Hazard, S., 3rd, Duzic, E., and Lanier, S. M. (1999) *J. Biol. Chem.* **274,** 33202–33205
6. Bernard, M. L., Peterson, Y. K., Chung, P., Jourdan, J., and Lanier, S. M. (2001) *J. Biol. Chem.* **276,** 1585–1593
7. Blumer, J. B., Chandler, L. J., and Lanier, S. M. (2002) *J. Biol. Chem.* **277,** 15897–15903
8. Cao, X., Cismowski, M. J., Sato, M., Blumer, J. B., and Lanier, S. M. (2004) *J. Biol. Chem.* **279,** 27567–27574
9. Sato, M., Cismowski, M. J., Toyota, E., Smrcka, A. V., Lucchesi, P. A., Chilian, W. M., and Lanier, S. M. (2006) *Proc. Natl. Acad. Sci. U. S. A.* **103,** 797–802
10. Peterson, Y. K., Bernard, M. L., Ma, H., Hazard, S., 3rd, Graber, S. G., and Lanier, S. M. (2000) *J. Biol. Chem.* **275,** 33193–33196
11. De Vries, L., Fischer, T., Tronchere, H., Brothers, G. M., Strockbine, B., Siderovski, D. P., and Farquhar, M. G. (2000) *Proc. Natl. Acad. Sci. U. S. A.* **97,** 14364–14369
12. Natochin, M., Lester, B., Peterson, Y. K., Bernard, M. L., Lanier, S. M., and Artemyev, N. O. (2000) *J. Biol. Chem.* **275,** 40981–40985
13. Bellaiche, Y., Radovic, A., Woods, D. F., Hough, C. D., Parmentier, M. L., O'Kane, C. J., Bryant, P. J., and Schweisguth, F. (2001) *Cell* **106,** 355–366
14. Colombo, K., Grill, S. W., Kimple, R. J., Willard, F. S., Siderovski, D. P., and Gonczy, P. (2003) *Science* **300,** 1957–1961
15. Du, Q., Stukenberg, P. T., and Macara, I. G. (2001) *Nat. Cell Biol.* **3,** 1069–1075
16. Gotta, M., Dong, Y., Peterson, Y. K., Lanier, S. M., and Ahringer, J. (2003) *Curr. Biol.* **13,** 1029–1037
17. Kaushik, R., Yu, F., Chia, W., Yang, X., and Bahri, S. (2003) *Mol. Biol. Cell* **14,** 3144–3155
18. Pattingre, S., De Vries, L., Bauvy, C., Chantret, I., Cluzeaud, F., Ogier-Denis, E., Vandewalle, A., and Codogno, P. (2003) *J. Biol. Chem.* **278,** 20995–21002
19. Schaefer, M., Petronczki, M., Dorner, D., Forte, M., and Knoblich, J. A. (2001) *Cell* **107,** 183–194
20. Schaefer, M., Shevchenko, A., Shevchenko, A., and Knoblich, J. A. (2000) *Curr. Biol.* **10,** 353–362
21. Yu, F., Morin, X., Cai, Y., Yang, X., and Chia, W. (2000) *Cell* **100,** 399–409
22. Betschinger, J., and Knoblich, J. A. (2004) *Curr. Biol.* **14,** R674–R685
23. Willard, F. S., Kimple, R. J., and Siderovski, D. P. (2004) *Annu. Rev. Biochem.* **73,** 925–951
24. Bowers, M. S., McFarland, K., Lake, R. W., Peterson, Y. K., Lapish, C. C., Gregory, M. L., Lanier, S. M., and Kalivas, P. W. (2004) *Neuron* **42,** 269–281
25. Blumer, J. B., Kuriyama, R., Gettys, T. W., and Lanier, S. M. (2006) *Eur. J. Cell Biol.* **85,** 1233–1240
26. Du, Q., and Macara, I. G. (2004) *Cell* **119,** 503–516
27. Lechler, T., and Fuchs, E. (2005) *Nature* **437,** 275–280
28. Sanada, K., and Tsai, L. H. (2005) *Cell* **122,** 119–131
29. Sans, N., Wang, P. Y., Du, Q., Petralia, R. S., Wang, Y. X., Nakka, S., Blumer, J. B., Macara, I. G., and Wenthold, R. J. (2005) *Nat. Cell Biol.* **7,** 1179–1190
30. Siegrist, S. E., and Doe, C. Q. (2005) *Cell* **123,** 1323–1335
31. Wiser, O., Qian, X., Ehlers, M., Ja, W. W., Roberts, R. W., Reuveny, E., Jan, Y. N., and Jan, L. Y. (2006) *Neuron* **50,** 561–573
32. Yao, L., McFarland, K., Fan, P., Jiang, Z., Inoue, Y., and Diamond, I. (2005) *Proc. Natl. Acad. Sci. U. S. A.* **102,** 8746–8751
33. Yao, L., McFarland, K., Fan, P., Jiang, Z., Ueda, T., and Diamond, I. (2006) *Proc. Natl. Acad. Sci. U. S. A.* **103,** 7877–7882
34. Zigman, M., Cayouette, M., Charalambous, C., Schleiffer, A., Hoeller, O., Dunican, D., McCudden, C. R., Firnberg, N., Barres, B. A., Siderovski, D. P., and Knoblich, J. A. (2005) *Neuron* **48,** 539–545
35. Blumer, J. B., Bernard, M. L., Peterson, Y. K., Nezu, J., Chung, P., Dunican, D. J., Knoblich, J. A., and Lanier, S. M. (2003) *J. Biol. Chem.* **278,** 23217–23220
36. Siller, K. H., Cabernard, C., and Doe, C. Q. (2006) *Nat. Cell Biol.* **8,** 594–600
37. Izumi, Y., Ohta, N., Hisata, K., Raabe, T., and Matsuzaki, F. (2006) *Nat. Cell Biol.* **8,** 586–593
38. Yasumi, M., Sakisaka, T., Hoshino, T., Kimura, T., Sakamoto, Y., Yamanaka, T., Ohno, S., and Takai, Y. (2005) *J. Biol. Chem.* **280,** 6761–6765
39. Pizzinat, N., Takesono, A., and Lanier, S. M. (2001) *J. Biol. Chem.* **276,** 16601–16610
40. Nagase, T., Ishikawa, K., Suyama, M., Kikuno, R., Hirosawa, M., Miyajima, N., Tanaka, A., Kotani, H., Nomura, N., and Ohara, O. (1999) *DNA Res.* **6,** 63–70
41. Strausberg, R. L., Feingold, E. A., Grouse, L. H., Derge, J. G., Klausner, R. D., Collins, F. S., Wagner, L., Shenmen, C. M., Schuler, G. D., Altschul, S. F., Zeeberg, B., Buetow, K. H., Schaefer, C. F., Bhat, N. K., Hopkins, R. F., *et al.* (2002) *Proc. Natl. Acad. Sci. U. S. A.* **99,** 16899–16903
42. Raymond, J. R., Olsen, C. L., and Gettys, T. W. (1993) *Biochemistry* **32,** 11064–11073
43. Sheng, M., and Sala, C. (2001) *Annu. Rev. Neurosci.* **24,** 1–29

44. Chishti, A. H., Kim, A. C., Marfatia, S. M., Lutchman, M., Hanspal, M., Jindal, H., Liu, S. C., Low, P. S., Rouleau, G. A., Mohandas, N., Chasis, J. A., Conboy, J. G., Gascard, P., Takakuwa, Y., Huang, S. C., Benz, E. J., Jr., Bretscher, A., Fehon, R. G., Gusella, J. F., Ramesh, V., Solomon, F., Marchesi, V. T., Tsukita, S., Hoover, K. B., *et al.* (1998) *Trends Biochem. Sci.* **23,** 281–282
45. Diakowski, W., Grzybek, M., and Sikorski, A. F. (2006) *Folia Histochem. Cytobiol.* **44,** 231–248
46. Hung, A. Y., and Sheng, M. (2002) *J. Biol. Chem.* **277,** 5699–5702
47. Cho, W., and Stahelin, R. V. (2005) *Annu. Rev. Biophys. Biomol. Struct.* **34,** 119–151
48. Weiss, T. S., Chamberlain, C. E., Takeda, T., Lin, P., Hahn, K. M., and Farquhar, M. G. (2001) *Proc. Natl. Acad. Sci. U. S. A.* **98,** 14961–14966
49. Stow, J. L., de Almeida, J. B., Narula, N., Holtzman, E. J., Ercolani, L., and Ausiello, D. A. (1991) *J. Cell Biol.* **114,** 1113–1124
50. Petiot, A., Ogier-Denis, E., Bauvy, C., Cluzeaud, F., Vandewalle, A., and Codogno, P. (1999) *Biochem. J.* **337,** 289–295
51. Cho, H., and Kehrl, J. H. (2007) *J. Cell Biol.* **178,** 245–255
52. Sato, M., Gettys, T. W., and Lanier, S. M. (2004) *J. Biol. Chem.* **279,** 13375–13382
53. Adhikari, A., and Sprang, S. R. (2003) *J. Biol. Chem.* **278,** 51825–51832
54. Bompard, G., Martin, M., Roy, C., Vignon, F., and Freiss, G. (2003) *J. Cell Sci.* **116,** 2519–2530
55. Bohil, A. B., Robertson, B. W., and Cheney, R. E. (2006) *Proc. Natl. Acad. Sci. U. S. A.* **103,** 12411–12416
56. Letunic, I., Copley, R. R., Pils, B., Pinkert, S., Schultz, J., and Bork, P. (2006) *Nucleic Acids Res.* **34,** D257–D260